Plasma heating and improvement of lower hybrid current drive efficiency by electron cyclotron waves on EAST

Miaohui Li[1], *Handong* Xu[1*], *Xiaojie* Wang[1], *Mao* Wang[1], *Bojiang* Ding[1], *Weiye* Xu[1], *Dajun* Wu[1], *Yunying* Tang[1], *Liyuan Zhang*[1], *Zege* Wu[1], *Jian* Wang[1], *Tao* Zhang[1], *Hanlin* Wang[1], *Qing* Zang[1], *Hailin* Zhao[1], *Haiqing* Liu[1], *Jinping* Qian[1], *Xianzu* Gong[1], *Fukun* Liu[1] *and Xiaolan* Zou[2]

[1]Institute of Plasma Physics, Chinese Academy of Sciences, Hefei 230031, P. R. China
[2]CEA, IRFM, Saint Paul-lez-Durance, France

Abstract. The electron cyclotron (EC) system on EAST consists of four gyrotrons with a frequency of 140 GHz (second harmonic of the extraordinary mode), each of which is expected to deliver a maximum power of 1.0 MW and be operated at 100-1000 s pulse length. Significant progress in long-pulse operation has been achieved recently, including the pulse duration up to 1056 s with EC power injected into plasma of 0.55 MW and the pulse duration of 310 s with EC power of 1.6 MW (output by 3 gyrotrons). High electron temperature (T_e >12 keV) plasma measured by Thomson scattering was produced with the combination of EC and lower hybrid (LH) waves. It is found that the plasma heating effect depends on the EC power location greatly. By adjusting the EC power location, the plasma current profile can be modified. As a consequence of the increment of electron temperature by electron cyclotron resonance heating (ECRH), the lower hybrid current drive (LHCD) efficiency is improved, benefiting for the long-pulse operation. In addition, a synergy effect between EC and LH current drive was observed in steady-state operation on EAST.

1 Introduction

Electron cyclotron resonance heating (ECRH), as a highly efficient and controllable heating tool, has been widely used in tokamak magnetic confinement devices [1]. Usually, the EC power can be injected as narrow Gaussian beams, which gives rise to highly localized power deposition. Consequently, ECRH and electron cyclotron current drive (ECCD) are considered to be an effective tool to locally control the electron temperature and current profile in plasmas. An electron temperature (T_e) of up to 26 keV was achieved in JT-60U by injecting EC power of 2.9 MW into the centre of a reversed shear plasma produced by the lower hybrid (LH) waves [2]. EAST has four units of EC systems (No. 1– No. 4), each of which has one gyrotron with a frequency of 140 GHz (see Fig. 1) [3 - 5]. Additional two gyrotrons system is under development. However, the No. 1 gyrotron is currently undergoing repair (air leakage issue). EC waves are injected from the lower field side of the torus as an X-mode. In line with the long pulse operational capability of EAST, it is designed for a pulse length up to 1000 s. There are two high power lower hybrid current drive (LHCD) systems on EAST with different operating frequencies (2.45 GHz /4 MW, referred as LH1 [6] and 4.6 GHz /6 MW, referred as LH2 [7]). Both of the EC and LH systems are the main electron heating and current drive source for the long-pulse operation on EAST.

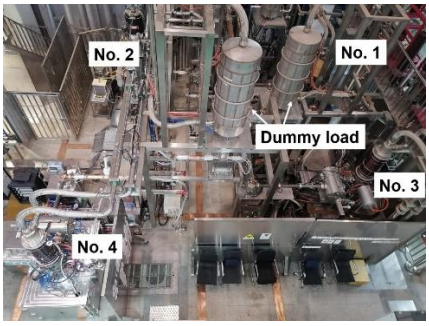

Fig. 1. Layout of ECRH system

2 Experimental results and analysis

2.1 progress in long-pulse and high T_e operation

The first EC system was installed on EAST in 2015 with one gyrotron and the EC wave injected into plasma was ~ 0.5 MW. Thanks to the continuous increase in the number of EC systems and the improvement of the system, significant progress in high-power and long-pulse operation has been achieved recently. As shown in Fig. 2, the pulse duration has been extended to ~ 1056 s with P_{EC} ~ 0.55 MW, corresponding to the EC energy injected into the plasma ~ 0.58 GJ. During this discharge, the EC power was shut down at 550 s, but it restarted automatically to work after 10 s (see Fig. 3). High power as 1.6 MW (output by 3 gyrotrons) injected into H-mode

* Corresponding author: xhd@ipp.ac.cn

plasmas with pulse duration ~ 310 s has been achieved. The increase in available input power made it possible to produce plasmas with high T_e of up to 12 keV, which is measured by Thomson scattering diagnostic (see Fig. 4). The peak electron temperature was increased from 6.5 keV to 12 keV when 1.4 MW EC adding to the plasmas sustained by 2.3 MW LH power.

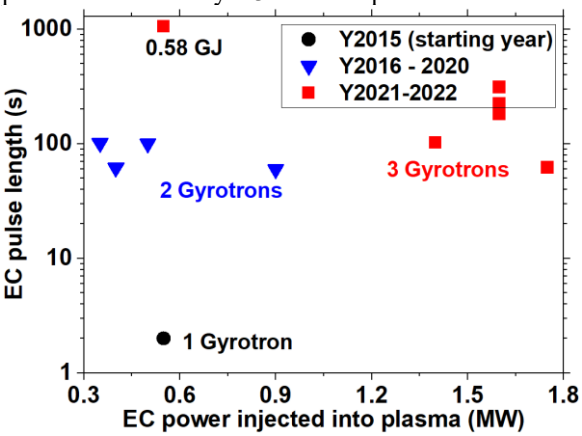

Fig. 2. Advances in the EC power injected into plasma and in their pulse duration on EAST.

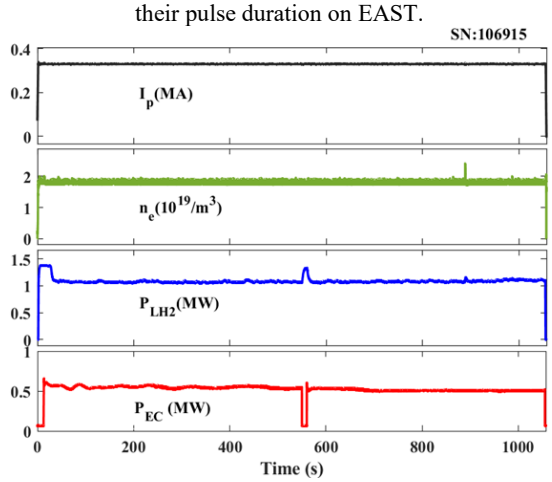

Fig. 3. A typical long-pulse discharge with duration up to 1056 s sustained by EC and LH waves.

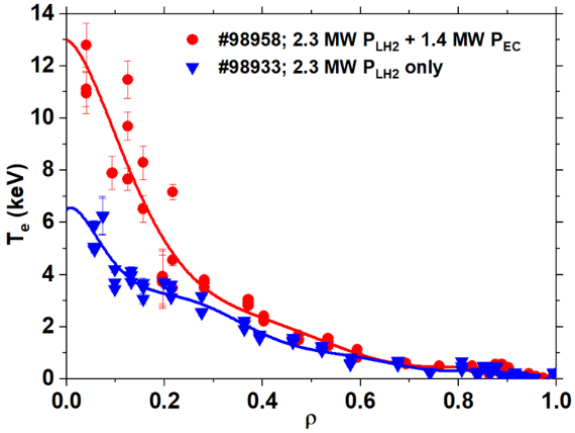

Fig. 4. Comparison of Electron temperature profiles measured by Thomson scattering with ECRH and without ECRH.

2.2 Effects of EC power location on plasma heating and current density profile

Each of the EC antennas consists of two mirrors located at the same port, one fixed focusing mirror and one movable plane mirror. The launching angle can be continuously varied with range of over 30 degrees in poloidal direction and ± 25 degrees in toroidal. Fig. 5 shows the increment of the plasma stored energy (W_{MHD}) and the central electron temperature when EC power injected into ohmic plasmas with different power deposition location realized by changing the poloidal angle. It is seen that an on – axis power deposition is critical for effective heating.

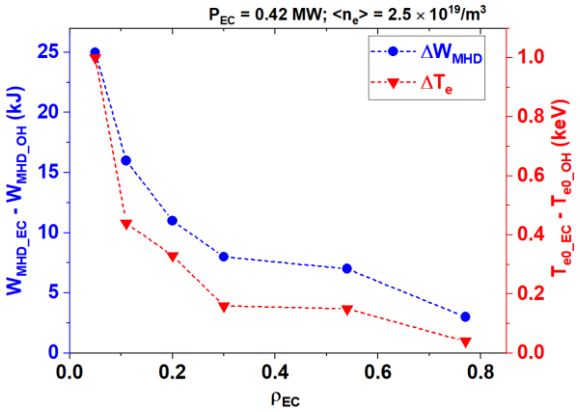

Fig. 5. The increment of plasma stored energy and central electron temperature after EC power injection versus EC power deposition location.

Shaping of the current density profiles by adjusting the EC power deposition is demonstrated. As shown in Fig. 6, when the EC power shifts from ρ ~ 0.03 to 0.3, the internal inductance (l_i) is decreased by ~ 0.3, indicating an off-axis ECRH is helpful to broaden the current profile. The power density profiles calculated by TORAY code are plotted in Fig. 7. This conclusion is further verified by the polarimeter /interferometer (POINT) measurement [8, 9] as illustrated in Fig. 8. The Faraday rotation angle is propotional to $\int n_e(z)\, B_{||}(z) dz$, where $B_{||}$ is the magnetic field component along the laser beam and dz is the plasma path length. Since

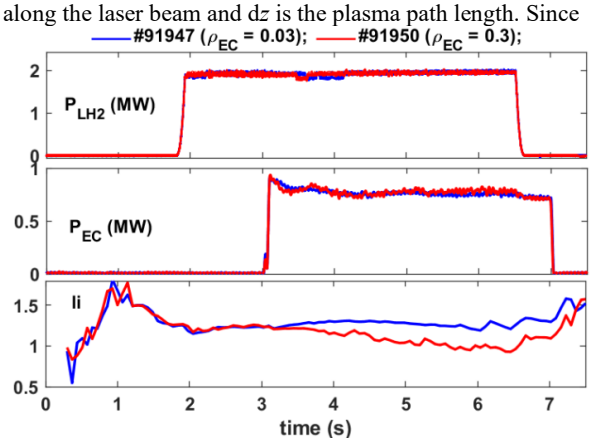

Fig. 6. Waveform of current density profiles modified by adjusting the EC deposition in LHCD sustained plasmas.

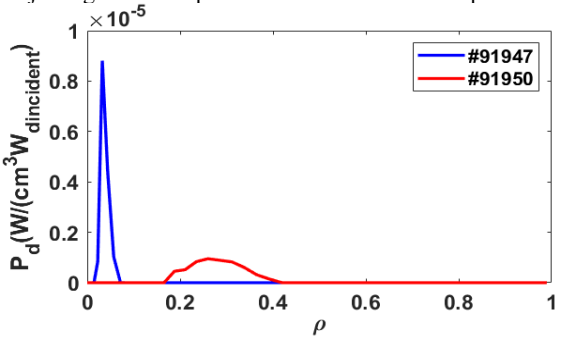

Fig. 7. Normalized power density profiles calculated with TORAY code

the density profiles are almost the same for these two discharges, the difference in Faraday rotation angle should be as a result of the different plasma current density profiles.

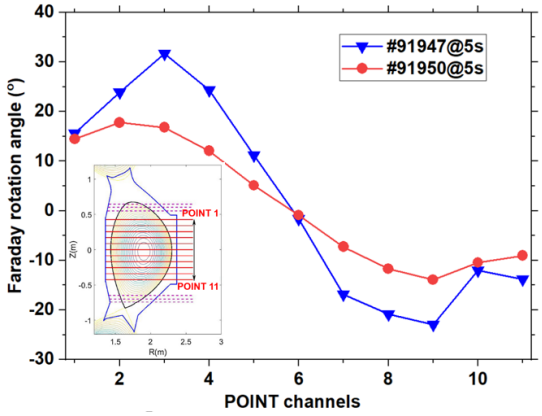

Fig. 8. Line-integrated Faraday rotation angle versus channels measured by POINT diagnostic. The optical layout of the 11 channels is also shown.

2.3 LHCD efficiency improved by ECRH

LHCD efficiency defined by

$$\eta = \frac{I_{\mathrm{LH}} n_e R}{P_{\mathrm{LH}}} (\mathrm{A/W}/m^2) \qquad (1),$$

is recognized as a key factor for dimensioning an LH system, where I_{LH} is the plasma current driven by LH wave, and R is the major radius of the plasma. According to the CD theory [10], LHCD efficiency increases with the square of the parallel resonant velocity, which is about 3.5 times of the thermal velocity $\upsilon_{\mathrm{th}} = \sqrt{kT_e/m_e}$. The experimental results also demonstrated that the LHCD efficiency is a significantly increasing function of $<T_e>$ [11, 12].

Fig. 9 shows a typical discharge of LHCD efficiency improved by ECRH. With the EC power of 0.3 MW heating in the plasma core, the central electron

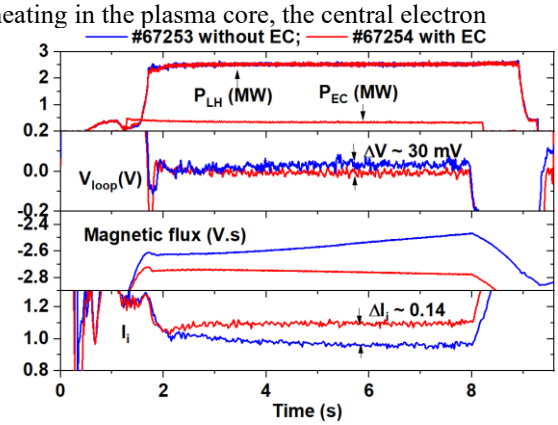

Fig. 9. Typical waveform of LHCD efficiency improved by ECRH.

temperature is increased by ~ 1.6 keV (see Fig. 10), leading to a higher CD efficiency indicated by a lower loop voltage (~ 30 mV). Moreover, a higher internal inductance (l_i) indicates that the LH current shifts to the inner region for the case with ECRH. Fig. 11 shows the LHCD efficiency with and without ECRH versus plasma density. Quasi-steady-state (V_{loop} < 100 mV) discharges are selected and the LH driven current is calculated by $I_{\mathrm{LH}} = I_{\mathrm{P}} - I_{\mathrm{EC}} - I_{\mathrm{OH}} - I_{\mathrm{BS}}$. It is seen that for similar density the LHCD efficiency in the plasmas with ECRH is higher by ~ 20% than that without ECRH. Besides, good CD effect (η ~ 0.9 × 10^{19}A/W/m^2) is obtained with the combination of LHCD and ECRH even when density increases up to 5.4 × 10^{19}/m3.

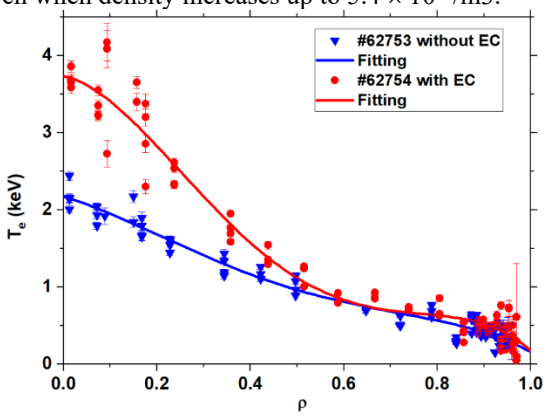

Fig. 10. Comparison of electron temperature profiles with and without ECRH.

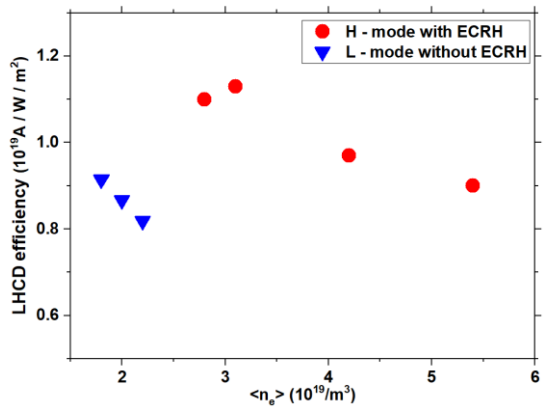

Fig. 11. Comparison of LHCD efficiency with and without ECRH.

It is well known that the interaction mechanism for EC waves with electrons is cyclotron damping, which accelerate electrons mainly in perpendicular direction; while for LH waves, it is dominant by Landau damping, which accelerates electrons mainly in parallel direction. When these two waves are injected simultaneously, if the particles accelerated by the EC waves reach the lowest limit velocity of the LH waves, or the EC power absorbed by the fast electron tail driven by the LH waves, a synergy effect between LHCD and ECCD will be created [13, 14]. This synergy effect was quantitatively demonstrated in steady-state experiments on Tore-Supra for the first time [15]. On EAST, the synergy effect between ECCD and LHCD is also observed in steady-state operation. The results obtained are well illustrated by the time history of discharge #106904, shown in Fig. 12. During this experiment, the LH power is feedback controlled by the magnetic flux consumption with constant plasma current (I_{p} = 320kA) and constant density (n_{e} = 1.8 × 10^{19}/m^3), which is similar to the previous experiment on Tore Supra [15]. Due to the faulty algorithm, the magnetic flux consumption is not controlled constantly during the LH alone phase. However, from phase 1 and phase 2, we can infer that for fully non-inductive LHCD (V_{loop} = 0), it needs LH power of (P_{LH}) 1.28 MW approximately with parallel refractive index $N_{\|}$ ~ 2.04. During the application of 0.55 MW ECCD with $N_{\|}$ ~ 0.34, the LH power drops (ΔP_{LH}) by approximately 0.3 MW (from 1.28 MW to 0.98 MW).

The bootstrap current (I_{BS}) calculated by Sauter model [16] is about 71 kA and the EC driven current calculated by TORAY code is in the range of 26 - 29 kA based on the measured electron and density profiles. Since the plasma current is kept constant and the loop voltage is zero, the additional current ΔI, driven by the EC waves in the presence of LH waves can be obtained by the formula

$$\Delta I = (I_p - I_{BS})\frac{\Delta P_{LH}}{P_{LH}} \qquad (2).$$

For discharge #106904, the additional current ΔI is ~ 59 kA. Consequently, the synergy factor defined as $F_{syn} = \Delta I / I_{EC}$ is estimate to be ~ 2.1 ± 0.1. Although the temperature shows a small difference during ECCD and before ECCD phases, this difference is not quantitatively large enough to explain the increase of the efficiency. As shown in Fig. 13, the ECE electron temperature during ECCD phase is only higher by ~ 5% than that before ECCD, while the LHCD efficiency is increased by 16% with the assumption that this part current ΔI - I_{EC} is driven by LH wave.

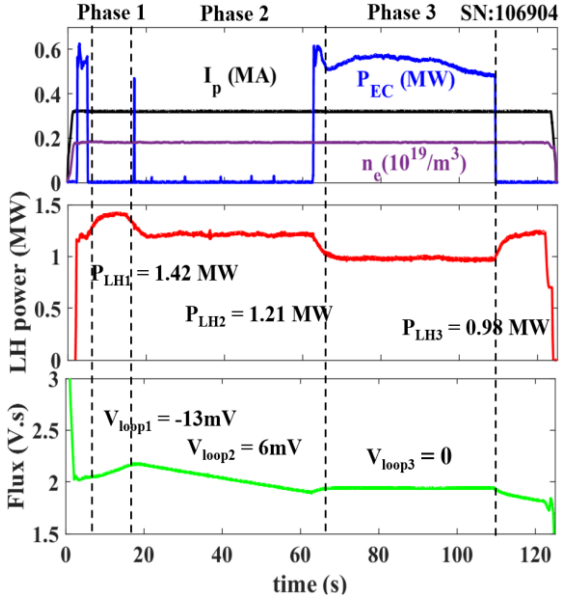

Fig. 12. The time history of a discharge during which the synergy effect between LHCD and ECCD is observed.

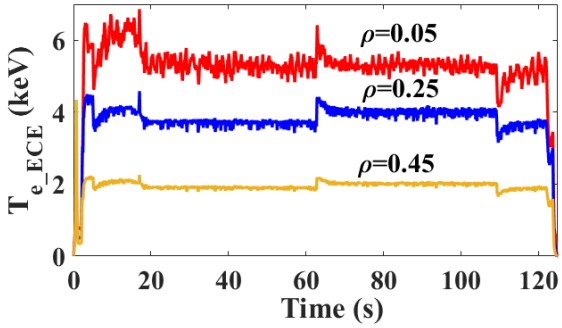

Fig. 13. Electron temperature measured by electron cyclotron emission (ECE) at various positions.

3 Summary and next work

With optimization of the operation conditions and improvement of the system, significant progress in long-pulse and high-power operation has been achieved with EC system, including pulse duration extended to ~ 1056 s with P_{EC} ~ 0.55 MW, and pulse duration ~ 310 s with P_{EC} up to 1.6 MW. High T_{e0} ~ 12 keV plasmas was maintained for 100 s by the combination of 1.4 MW EC and 2.3 MW LH power. Thanks to a higher electron temperature in the plasma core with ECRH, the LH power deposition shifts to the inner region, thus giving a higher LHCD efficiency. A synergy effect between ECCD and LHCD was observed in steady-state plasmas. TORAY modelling predicts that the ECCD current can be > 80 kA at low density as shown in Fig. 14. Next work will investigate the ECCD efficiency and the synergy effects with different $N_{||}$ of LH waves.

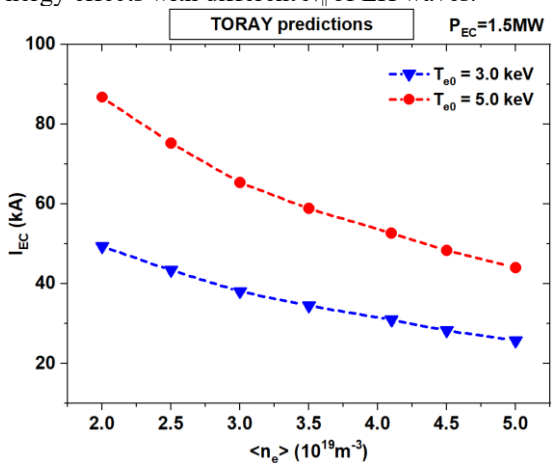

Fig. 14. Predicted ECCD current with different electron temperature and density.

Acknowledgement

This work was supported by the Performance Improvement Project of EAST, Hefei Comprehensive National Science Centre, the National Key R&D Program of China (Grant No. 2017YFE0300401) and the National Natural Science Foundation of China (Nos. 11305211 and 11775259). The authors would like to thank the experts from GYCOM and CPI companies for their great efforts in the development of gyrotrons for EAST.

References

1. ITER Physics Expert Group on Energetic Particles, Chapter 6: Plasma auxiliary heating and current drive, Nucl. Fusion **39**, 2495 (1999).
2. T. Suzuki et al., Nucl. Fusion **44**, 699 (2004).
3. H.D. Xu et al., Plasma Sci. Technol. **18**, 442 (2016).
4. X.J. Wang et al., Fusion Eng. Des **96-97**, 181 (2015).
5. H.D. Xu et al., Fusion Eng. Des.**164**, 112222 (2021).
6. J.F. Shan et al, *A New 4 MW LHCD System for EAST*, in Proceedings of the 23rd IAEA Fusion Energy Conference, Daejon, Korea (2010).
7. F.K. Liu et al., Fusion Engineering and Design **113**, 131 (2016).
8. H.Q. Liu et al., Rev Sci Instrum **87**, 11D903 (2016).

9. J.P. Qian et al., Nuclear Fusion **57**, 036008 (2017).
10. N.J. Fisch, Phys. Rev. Lett. **41**, 873 (1978).
11. K. Ushigusa et al., Nucl. Fusion **29**, 1052 (1989).
12. V. Pericoli Ridolfini et al., Phys. Rev. Lett. **82**, 93 (1999).
13. I. Fidone et al., Nucl. Fusion **27**, 579 (1987).
14. R. Dumont et al., Phys. Plasmas **7**, 4972 (2000).
15. G. Giruzzi, et al., Phys. Rev. Lett. **93**, 255002 (2004).
16. O. Sauter et al., Phys. Plasmas **6**, 2834 (1999)